SPATIO-TEMPORAL MODELING OF PARTICULATE MATTER CONCENTRATIONS INCLUDING COVARIATES

Ijaz Hussain[1,2], Hannes Kazianka[3], Jürgen Pilz[1]and Muhammad Faisal[4]
[1]Department of Statistics, University of Klagenfurt, 9020 Klagenfurt, Austria
[2]Department of Statistics, Quaid-i-Azam University, Islamabad, Pakistan
[3]Financial and Actuarial Mathematics, Vienna University of Technology,
Wiedner Hauptstrasse 8 / 105-1, 1040 Vienna, Austria
[4]Department of Bioinformatics, Quaid-i-Azam University, Islamabad, Pakistan
[2]ihussain@edu.uni-klu.ac.at

ABSTRACT: *Modeling the spatio-temporal distribution and characteristics of particulate matter remains a focal point of research. In the present study we model the spatio-temporal structure of* PM_{10} *with and without a spatial trend made of environmental covariates. (i) Spatio-temporal interpolation without accounting for covariates is done by using ordinary space-time kriging. (i) To include covariates into the model we propose the following methodology, a combination of methods that has not been investigated before: generalized additive regression is employed to capture the effects of the covariates by partitioning the output into a trend and a residual component. Furthermore, the unknown trend components at ungauged locations are estimated by spatial artificial neural networks and the corresponding residual components are predicted by means of ordinary space-time kriging based on a nested spatio-temporal covariance function that is optimized by a particle swarm algorithm. The results of both methods (i and ii) are compared by means of cross validation and it is found that the new methodology which takes the covariates into account performs significantly better, in particular, it yields a smaller mean squared error.*

Keywords: *Covariates, Nested space-time Covariance, SANN,Particulate matter andSpace-time Kriging*

1. INTRODUCTION

Earlier research [(1)& (3)] indicates that particulate matter (PM) concentration is related to thousands of deaths and regarded as a widespread health problem. Amongst others, the Environmental Protection Agency (EPA) of the United States of America is interested to understand the characteristics of PM. EPA scientists continue to conduct research related to the adverse health effects of PM by performing clinical studies and using the methods of epidemiology and toxicology. [14] proposed a random effects model for $PM_{2.5}$ concentrations. They introduce two random effects components, one for rural or background levels and the other as a supplement for urban areas and specified as spatio-temporal processes. They analyzed daily $PM_{2.5}$ concentrations in three midwestern U.S. states for the year 2001. [16] used a Geographic Information System (GIS) based spatial smoothing model to predict monthly outdoor PM_{10} concentrations in the northeastern and midwestern U.S. This model included monthly smooth spatial terms and smooth regression terms of GIS-derived and meteorological predictors. [5] compared space-time kriging with spatial kriging to predict an outpatient malaria data set and concluded that space-time kriging prediction produces more precise results than spatial kriging.

Amongst others [6, 7] showed that it may be beneficial to include information about covariates, e.g. environmental variables, into classical space-time interpolation models by analyzing precipitation in Pakistan during the Moonson season. Specifically in case of PM, [13] developed a conceptually simple spatio-temporal model which is also able to account for the effects of covariates. It has the ability to capture space-time interaction through the use of monthly varying spatial surfaces on large scale spatial heterogeneity. One limitation of their model, however, is that it cannot be used to predict the values of the response variable at unobserved locations when information about the covariates is missing.

The present paper extends the existing methodology by proposing to estimate the unknown covariates at ungauged locations first and to use them for spatio-temporal prediction subsequently presented in [8]. We apply a generalized additive regression model and estimate the unknown trend components by a spatial artificial neural network. Prediction of the residual components is then performed by ordinary space-time kriging and fitting a separable nested space-time covariance function using a particle swarm optimization algorithm.

The paper is organized as follows. Section 2 presents the proposed methodological framework and the study data set. Section 3 includes the study results and compares the proposed approach for spatio-temporal interpolation of PM_{10} with classical ordinary space-time kriging, which is not capable of incorporating covariates. We conclude that the spatio-temporal interpolation including covariates clearly performs better, i.e. yields a significantly smaller root mean square error. Finally, Section 4 is devoted to discussions.

2 MATERIAL AND METHODS

2.1 Study area

In the present study we consider the PM_{10} mass concentration data used by [13] and [16] with Northern U.S. as the spatial domain. In their study PM_{10} data were recorded from 922 sites but due to missing observations at most of the sites, we consider only those 61 sites in the same spatial domain where monthly concentrations for the years 1998-2002 were completely recorded. The distribution of

spatial locations is shown in Fig. 1. Temperature, wind speed, precipitation and the logarithm of area-source emissions of PM10 in short tons per year of the county that the monitoring site is within (logAreaEmit10) are considered as covariates.

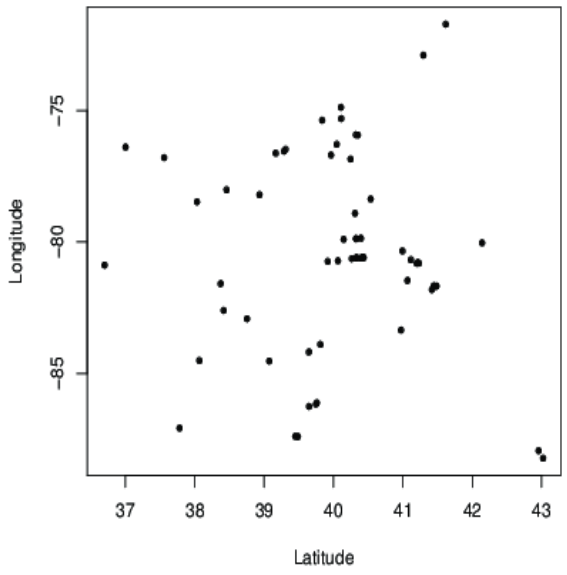

Figure 1: The distribution of gauged locations in the study data set.

2.2 Space-time model

Classical space-time models assume that the response variable is normally distributed. Since the distribution of PM_{10} is always skewed and positive, we apply the Box-Cox transformation to fulfill the assumption of normality. Let $\mathbf{Z}(s,t)$ denote the response variables at location s and time t, and let $\mathbf{Y}(s,t)$ be the Box-Cox transformed responses, respectively, i.e.

$$Y(s,t)=\begin{cases}\dfrac{\left(\mathbf{Z}^{\lambda}(s,t)-1\right)}{\lambda} & :\lambda\neq 0\\ log\left(\mathbf{Z}(s,t)\right) & :\lambda=0\end{cases}$$

We make use of the decomposed space-time modeling approach suggested by [15],

$$Y(s,t)=\mu(s,t)+R(s,t), \quad (1)$$

where $\mu(s,t)$ is the trend component modeled as a deterministic function of the spatial location s and the time point t, and $R(s,t)$ is the residual component describing fluctuations around the mean. We propose to use the generalized additive regression model (GAM) described in [4] with Gaussian link function for estimating the space-time model Eq. 1. The resulting output is partitioned into a trend component and a residual component. The trend component can be assumed to be deterministic, it can vary with respect to time and space if the spatial and temporal covariates are included. In our case we model the trend component based on temperature, wind speed and precipitation as space-time covariates and logAreaEmit10 as a purely spatial covariate, .i.e.

$$\mu(s,t)=\beta_0+\sum_{i=1}^{k} f_i\left(X_i(s,t)\right),$$

where f_i are smooth arbitrary functions and $k=4$ represents the number of environmental and spatio-temporal covariates X_i, $i=1,\ldots,k$. The trend model $\mu(s,t)$ is deterministic implying that there is no interaction between spatial and temporal variation. For ungauged sites we propose to model $\mu(s,t)$ using a spatial artificial neural network (SANN) as proposed by [11]. The SANN is a combination of four layers: input layer, Gaussian Kernel Function (GKF) layer, summation layer and estimation layer. The relationship among the four layers is displayed in Fig. 2. Suppose we have N gauged sites whose trend component $\mu(s,t)$ is known and we want to estimate the trend component $\hat{\mu}(s,t)$ at ungauged sites. Let $s(s_1,s_2)\in\mathbf{R}^2$ in $\mu(s,t)$ represent the spatial coordinates longitude and latitude, respectively, and t the time point, then the input layer will be $\mu(s,t)$ with three nodes. The input layer passes through the GKF layer without weighting. The GKF layer has N nodes which consist of observed vectors $(s_j,t), j=1\ldots N$. The Gaussian kernel can be defined as activation output a_j,

$$a_j=\exp\left(-\frac{D_{s,j}^2}{2\sigma_{s,j}^2}\right),\ j=1,\ldots,N,$$

where $D_{s,j}^2=(s-s_j)^T(s-s_j)$ is the distance of the j^{th} input vector from the corresponding node center s and $\sigma_{s,j}^2$ is the width or smoothing parameter which defines the respective field of influence of the regions for weighting of neighbor points for each GKF node. The parameter $\sigma_{s,j}^2$ depends on the number of neighboring points and the control factor F, which determines the density of the network. The parameter $\sigma_{s,j}^2$ can be estimated by the ratio of the root mean squared distance, $RMSD_s$, of the K (nearest neighbors) and the control parameter F, i.e

$$RMSD_{s_j}=\left(\frac{1}{K}\sum_{i=1}^{K}(s_i-s_j)^T(s_i-s_j)\right)^{\frac{1}{2}},\ j=1,\ldots,N,$$

where s_i is the i^{th} nearest neighbor point from the center of s_j, the j^{th} GKF node. Now the smoothing parameter can be determined as

$$\sigma_{s,j}^2=\frac{RMSD_{s_j}}{F},\ j=1,\ldots,N.$$

The summation layer is a combination of two nodes. The output of GKF nodes passes to the summation layer through weighted connections:

$$G_1 = \sum_{j=1}^{N}\left(\frac{1}{\sigma_{s,j}^2}\right)a_j \quad (2)$$

$$G_2 = \sum_{j=1}^{N}\left(\frac{1}{\sigma_{s,j}^2}\right)\mu(s_j,t)a_j \quad (3)$$

Finally, the output layer is the ratio of G_2 and G_1 obtained from the summation layer, i.e.

$$\hat{\mu}(s,t) = \frac{G_2}{G_1}.$$

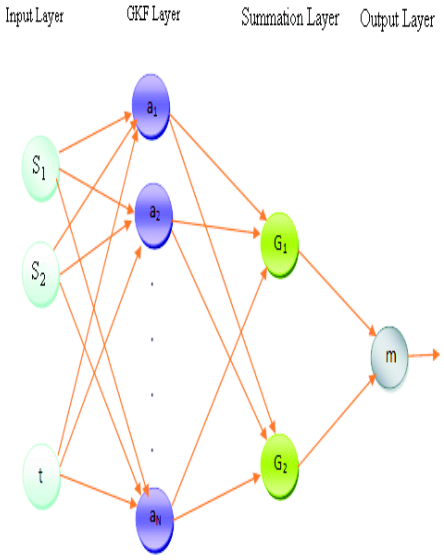

Figure 2: The structure of the spatial artificial neural network.

2.2.1 Spatio-temporal covariance modeling

The nested spatio-temporal covariance model proposed by [17] can be written as a linear combination of separable purely spatial and purely temporal covariance models which describe the dependence of the residual components at multiple scales of space and time:

$$C_{st}(h,\tau;\theta) = \sum_{l=1}^{L} b_l Cs(h;\theta_s)Ct(\tau;\theta_t). \quad (4)$$

Here Cs and Ct are permissible correlation functions at purely spatial and temporal domains with sills b_l, $l = 1,\ldots,L$. The particle swarm optimization (PSO) [9] algorithm is used to select an appropriate combination of permissible covariance models. PSO is used to solve non-linear optimization problems in many research fields, it depends only on the objective function to select optimal solutions from the given velocity and the solution space. The particle d represents a feasible solution and $x_{i,d}$ is the solution space which moves with varying velocity $v_{i,d}$. The PSO starts from a group of random solutions and iteratively searches for optimal solutions. In each iteration every particle is updated by following the best nearest neighbor solution $p_{i,d}$ and the global best solution $p_{g,d}$. After finding $p_{i,d}$ and $p_{g,d}$ the particle updates its velocity and positions as follows

$$v_{i+1,d} = v_{i,d} + c_1U_1(p_{i,d} - x_{i,d}) + c_2U_2(p_{g,d} - x_{i,d}),$$

$$x_{i+1,d} = x_{i,d} + v_{i+1,d},$$

where $v_{i+1,d}$ is the updated velocity of particle d and c_1 and c_2 are learning factors. Here, U_1 and U_2 are random numbers drawn uniformly from the unit interval. For fitting a covariance model using the PSO algorithm we consider the following weighted least squares criterion proposed by [2] as an objective function in PSO:

$$WLS(\theta) = \sum_{i=1}^{H}\sum_{j=1}^{T} \frac{N(h_i,\tau_j)\left(\hat{C}st(h_i,\tau_j) - Cst(h_i,\tau_j;\theta)\right)^2}{\left(\hat{C}s(0,0) - Cst(h_i,\tau_j;\theta)\right)^2},$$

where $\hat{C}st$ denotes the empirical covariance function and H and T define the number of spatial and temporal lags, respectively. Here the parameter vector θ includes the sills and the ranges for all separable structures in the space-time covariance function. Further, the number of parameters of the covariance model (Eq. 4) is chosen based on the Akaike Information Criterion (AIC). All possible nested models are sequentially tested and the one with lowest AIC value is selected.

2.3 Space-time kriging

The major aim in (space-time) geostatistics is typically to predict the value of $Y^*(s_0,t_0)$ at unobserved locations s_0 and unobserved time t_0 based on the observed data $Y(s_i,t_i)$, $i = 1,\ldots,n$, where (s_i,t_i) represents the vector of spatio-temporal coordinates and n is the number of observed locations/time points. The value of $Y^*(s_0,t_0)$ can be predicted by kriging as originally developed by [12] for purely spatial domains, and which was modified by [10] to incorporate the data distributed through spatial and temporal domains. For predicting the value of $Y(s_0,t_0)$ at an unobserved location and/or time point, a linear predictor is used, i.e.

$$Y^*(s_0,t_0) = \sum_{i=1}^{n}\lambda_i(s_i,t_i)Y(s_i,t_i), \quad (5)$$

where $\sum_{i=1}^{n}\lambda_i(s_i,t_i) = 1$ assures unbiasedness. For estimating the optimum weights, space-time kriging minimizes the prediction variance while implicitly taking account of the covariances between observed and unobserved locations and time points:

$$\sigma^2(s_0,t_0) = E\left(Y^*(s_0,t_0) - Y(s_0,t_0)\right)^2 \quad (6)$$

3 Study Results

This section presents the results for parameter estimation and spatio-temporal prediction of the PM_{10} data set introduced in Section 2.1 under the model proposed in Sections 2.2-2.3. Moreover, these results are compared to those of classical ordinary space-time kriging.

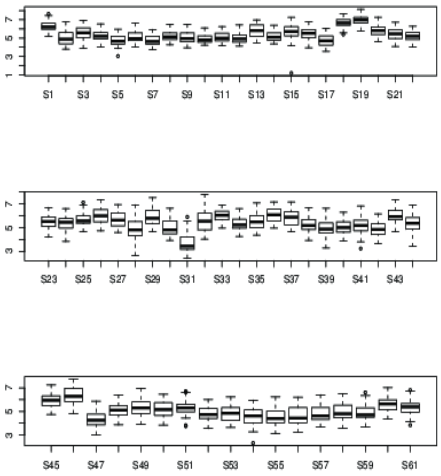

Figure 3: Boxplot of the Box-Cox transformed PM_{10} measurements at each location.

3.1 Parameter estimation results

Since the PM_{10} data is positively skewed, the Box-Cox transformation is applied to normalize the data and the transformation parameter λ is estimated as $\lambda = 0.3$. The boxplots of the transformed data are shown in Fig. 3. The generalized additive regression model is used to capture the influence of covariates on PM_{10}. The partial effect of covariates on PM_{10} is displayed in Fig. 4. The black dots represent the individual partial residuals of the covariates whereas lines represent the smoothed partial effect of the covariate on the response variable. The shaded red colored area represents the corresponding 95% credible interval.

The nested separable spatio-temporal covariance model estimated using the PSO algorithm for the transformed

$$C(h,\tau) = c_1 \exp\left(-\frac{3h}{a_{r_1}}\right)\exp\left(-\frac{3\tau}{a_{t_1}}\right) + c_2 \exp\left(-\frac{3h^2}{a_{r_2}^2}\right)\exp\left(-\frac{3\tau}{a_{t_2}}\right), \quad (7)$$

PM_{10} and for the residual components resulting from the GAM (Eq. 1) are shown in Eq. 7 and Eq. 8, respectively. The fitted nested covariance model contains two structured separable spatio-temporal covariance models for covariance modeling of transformed PM_{10} i) spatial exponential and temporal exponential ii) spatial Gaussian and temporal exponential. The residual covariances model also consist of two structured models i) exponential spatial and exponential temporal ii) exponential spatial and Gaussian temporal. The fitted spatio-temporal covariance functions for transformed PM_{10} and the residual component are shown in the left and right panel of Fig. 5, respectively.

$$C(h,\tau) = c_1 \exp\left(-\frac{3h}{a_{r_1}}\right)\exp\left(-\frac{3\tau}{a_{t_1}}\right) + c_2 \exp\left(-\frac{3h}{a_{r_2}}\right)\exp\left(-\frac{3\tau^2}{a_{t_2}^2}\right), \quad (8)$$

where $c_1 = 0.27$ and $c_2 = 0.42$ are the corresponding sills, $(a_{r_1}, a_{r_2})^T = (44.38, 2.44)^T$ and $(a_{t_1}, a_{t_2})^T = (0.63\ months, 232.82\ months)^T$ are the spatial and temporal ranges. The covariance models fitted for the residual components have sills $c_1 = 0.29$ and $c_2 = 0.16$. The corresponding spatial and temporal ranges are $(a_{r_1}, a_{r_2})^T = (2.42, 9.52)^T$ and $(a_{t_1}, a_{t_2})^T = (395.03\ months, 1.7153\ months)^T$, respectively.

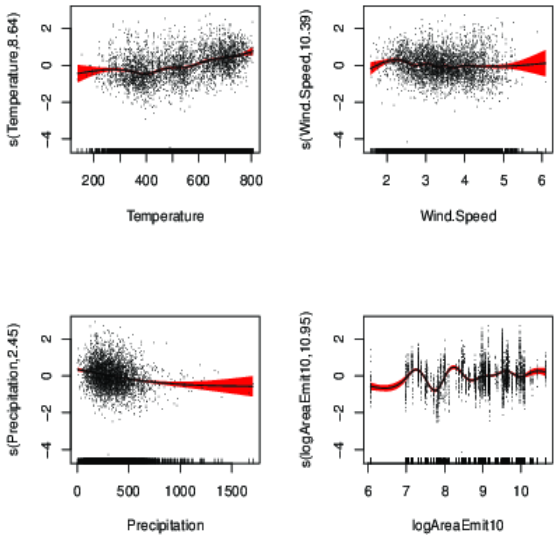

Figure 4: The effect of covariates on PM_{10} for gauged locations. The title of the y-axis contains the name of the smoothed covariate together with the respective bandwidth at which it was smoothed.

Furthermore, the trend components, i.e. the unknown values of the covariates, are estimated using the SANN. Thirty sites are considered as observed training points, while the remaining thirty-one sites are treated as unknown and are re-estimated. For every month under consideration vectors of. Ordinary space-time kriging excluding covariates is also performed for the ungauged locations based on the fitted covariance model of transformed PM_{10} and different values for control parameter F and nearest neighbor points K are used for training data. The optimal values of the control parameter F, the number of nearest neighbor points K and corresponding minimum mean squared error are presented in Table 1. The program to perform training and estimation is provided with supplementary material. Furthermore, the residuals at the ungauged locations are predicted with the help of ordinary space-time kriging and are added to the respective estimated trend values. The resulting predictions in the Gaussian space are then back-transformed to the original scale using the inverse Box-Cox

transformationthen back-transformed to the original scale. Note, that applying the inverse Box-Cox transformation as the back-transformation method inplies that the estimator for PM_{10} is the median and not the mean of the predictive distribution. Approximating the mean of the predictive distribution, e.g. by using the delta-method, would only be possible in case of ordinary space-time kriging. This is because the prediction variance in case of the alternative model including covariates is difficult to assess due to the use of the SANN. To guarantee a fair comparison, we decided to use the inverse Box-Cox transformation for both models.

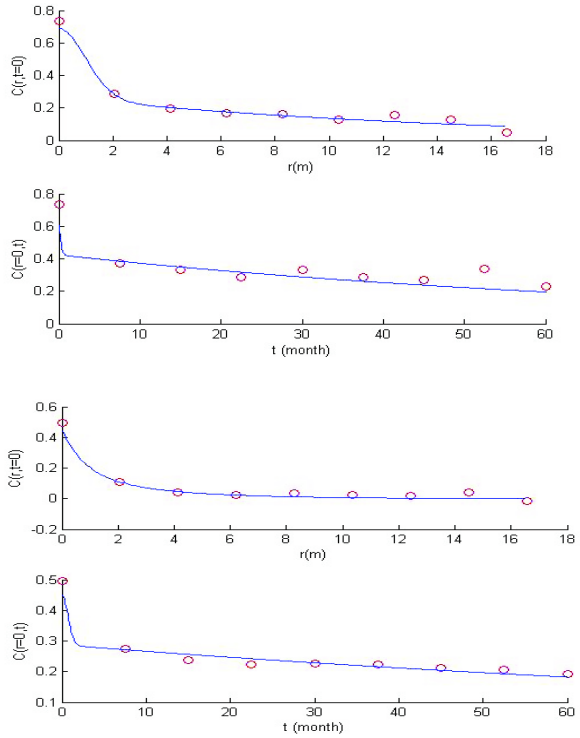

Figure 5: Empirical and theoretical spatio-temporal covariance function. Top panel: Box-Cox transformed PM10. Bottom panel: Residuals of the fitted GAM.

3.2 Space-time prediction results

The corresponding prediction maps are shown in Fig. 6 and Fig. 7. Overall, we find that the results for the model including covariates are more reliable, e.g. the maximum of all predicted values of the alternative model without covariates is about 150, while the largest observed value is only 61.5 which approximately corresponds to the results of the model that takes the covariates into account. Moreover, the prediction maps corresponding to the interpolation excluding covariates show more variation than those resulting from the model that takes into account the covariate information.

As a quantitative method for model comparison we employ leave-one-out cross validation. Table 2 shows the root mean squared prediction error (RMSPE) for both methods. It is observed that for most of the considered months the prediction method including covariates yields a significantly smaller RMSPE compared to the prediction without covariates. The coefficient of determination, R^2, for the model including covariates is 47% whereas for the model without covariates this value is only 6%. The sigificant increase in R^2 and the smaller RMSPE indicate that the model including covariates performs significantly better.

Figure 8 displays the approximate ordinary space-time kriging prediction variance for January estimated by the delta-method. The results for all the other months are very similar. The delta-method, in this case, proceeds as follows:

$$\widehat{Var}(Z_{(s_0,t_0)}) = \sigma^2(s_0,t_0)(\hat{\lambda}Y^*(s_0,t_0)+1)^{2\hat{\lambda}-2},$$

where $\hat{\lambda} = 0.3$, $Y^*(s_0,t_0)$ is the ordinary space-time kriging predictor in the transformed (Gaussian) space (Eq. 5) and $\sigma^2(s_0,t_0)$ is the corresponding prediction variance (Eq. 6). As already thematized, it is difficult to estimate the prediction variance for the proposed method, which also predicts the covariates, because of the additional uncertainty induced by the SANN. Approximate inference is possible, e.g. by applying a bootstrap procedure and analyzing the resulting bootstrap distribution. However, bootstrapping is a very time-consuming alternative, which is why it has not been employed in this study.

4 DISCUSSION

The present paper compares two spatio-temporal interpolation methods that can be employed to predict PM_{10}. The first one is ordinary space-time kriging which does not have the possibility to take unknown covariates at unobserved locations into account. The second method, which we propose in this paper, estimates the covariates using a spatial artificial neural network in combination with generalized additive regression. It is observed that the novel model not only leads to a smaller root mean squared error compared to the model without covariates but also suits the data better from a qualitative perspective. The prediction maps presented in Fig. 6 show that the behavior of PM_{10} changes temporally. The amount on PM_{10} remains very low in the month of February and very high in months of June and July. Moreover, it can be concluded that during the winter season from December to April the amount of PM_{10} gets lower, whereas in the summer season it gets higher, which shows that temperature has a major impact on PM_{10}. The spatial behavior of PM_{10} remains similar throughout the year.

The proposed method has the benefit that it is able to interpolate the values of PM_{10} for any month and any location, even if the values of covariates are unknown. One of the disadvantages is that the prediction variance cannot be assessed easily. This remains one of the major issues for future research.

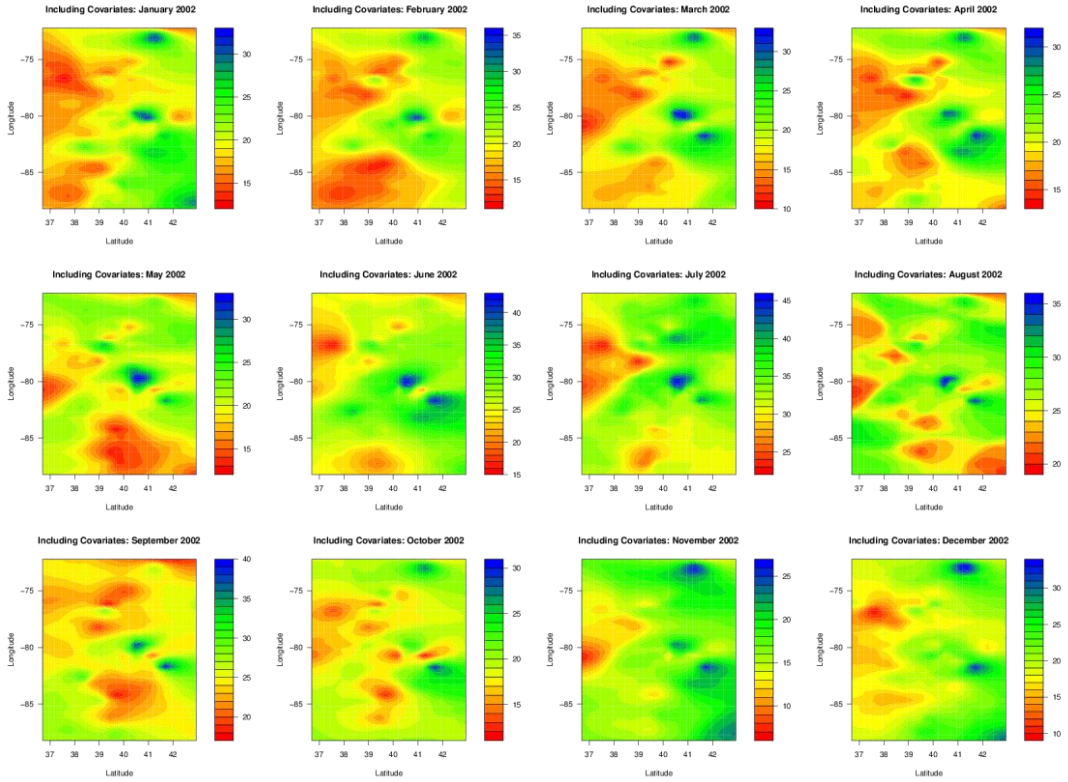

Figure 6: Prediction maps for PM_{10} resulting from the proposed model including covariates.

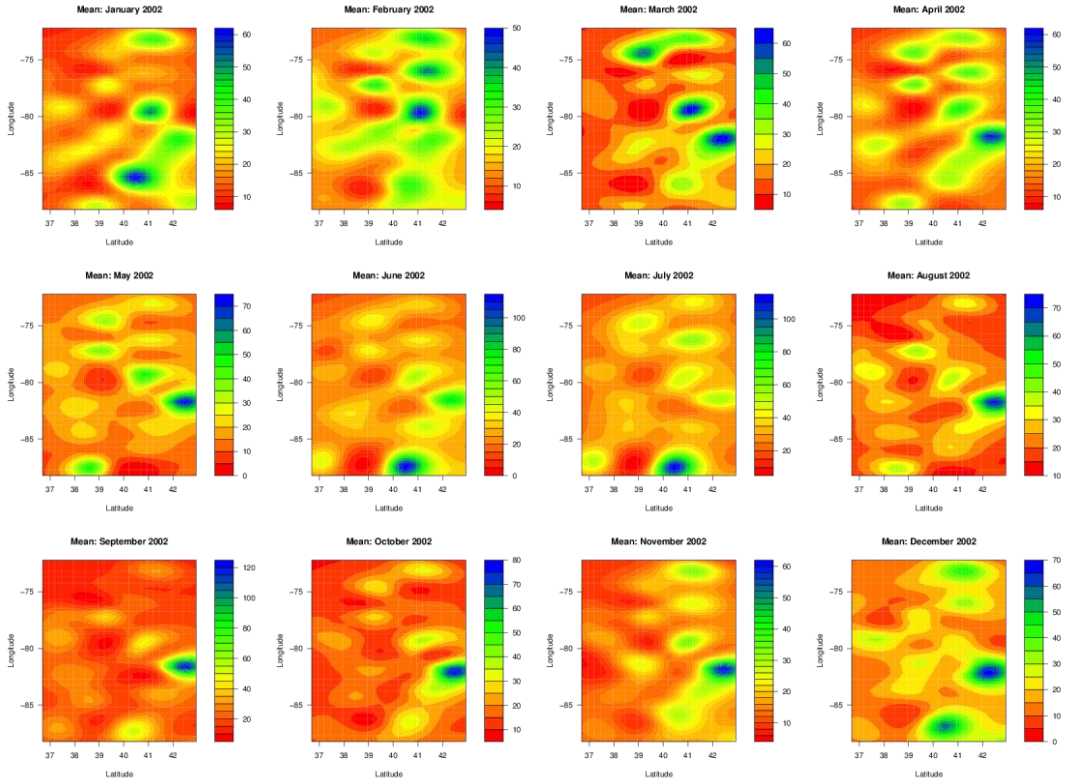

Figure 7: Ordinary space-time kriging prediction maps for PM_{10}

Table 1: SANN: Minimum mean square error and optimal parameter values for year 2002.

Parameters	Jan	Feb	Mar	Apr	May	June	July	Aug	Sep	Oct	Nov	Dec
F	1.7	2.3	1.9	2.2	1.7	1	1	2.4	1.5	0.8	2.1	0.7
K	5	9	9	9	5	5	5	4	9	7	9	5
MSE	0.28	0.28	0.30	0.26	0.32	0.26	0.27	0.32	0.28	0.22	0.27	0.28

Table 2: Root mean square cross-validation error corresponding to space-time kriging including and excluding covariates at ungauged locations.

Models	Jan	Feb	Mar	Apr	May	June	July	Aug	Sep	Oct	Nov	Dec	Mean
Incl.	5.82	6.39	6.34	6.34	5.42	5.96	4.59	6.24	7.39	5.71	4.88	6.59	5.97
Excl.	8.27	8.95	7.64	7.29	7.25	7.98	10.13	7.67	8.68	7.14	5.89	8.69	7.97

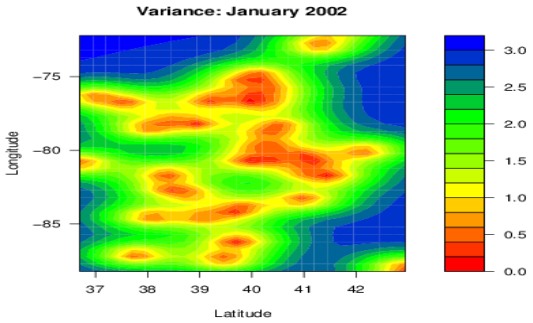

Figure 8: Ordinary space-time kriging prediction variance map for PM_{10}, January 2002.

REFERENCES

[1] Chuang, K.J., Yan, Y.H., Chiu, S.Y., & Cheng, T.J. Long-term air pollution exposure and risk factors for cardiovascular diseases among the elderly in Taiwan. *Occupational and Environmental Medicine*, **68**(1), 64–68(2011).

[2] Cressie, N. Fitting variogram models by weighted least squares. *Mathematical Geology*, **17**, 563–586(1985).

[3] Diez Roux, A.V., Auchincloss, A.H., Astor, B., Barr, R.G., Cushman, M., Dvonch, T., Jacobs, D.R., Kaufman, J., Lin, X., & Samson, P. (2006). Recent exposure to particulate matter and C-reactive protein concentration in the multi-ethnic study of atherosclerosis. *American Journal of Epidemiology*, 164(5), 437–448.

[4] Faraway, J.J. (2006). *Extending the linear model with R*. Boca Raton: Chapman & Hall/CRC.

[5] Gething, P.W., Atkinson, P.M., Noor, A.M., Gikandi, P.W., Hay, S.I., & Nixon, M.S. (2007). A local space-time kriging approach applied to a national outpatient malaria data set. *Computers & Geosciences*, 33, 1337–1350.

[6] Hussain, I., Spöck, G., Pilz, J., & Yu, H.L. (2010a). Spatio-temporal interpolation of precipitation during monsoon periods in Pakistan. *Advances in Water Resources*, 33(8), 880–886.

[7] Hussain, I., Pilz, J., & Spöck, G. (2010b). Hierarchical Bayesian space-time interpolation versus spatio-temporal BME approach. *Advances in Geosciences*, 25, 97–102.

[8] Hussain, I.,Spoeck, G., Pilz, G., Faisal, M., and Yu, H., (2012) "Spatio-Temporal Interpolation of Precipitation including covariates: during monsoon periods in Pakistan"Pakistan Journal of Statistics, Vol: 28(3), pp: 351-365.

[9] Kennedy, J., & Eberhart, R.C. (1995). Particle swarm optimization. IEEE International Conference on Neural Networks, 4, 1942–1948.

[10] Kyriakidis, P.C, & Journel, A.G. (1999). Geostatistical space-time models: A review. *Mathematical Geology*, 31(6), 651–684.

[11] Martinez, A., Salas, D.J., & Green, T.R. (2004). Sensitivity of spatial analysis neural network training and interpolation to structural parameters. *Mathematical Geology*, 36(2), 721–742.

[12] Matheron, G. (1963). Principles of geostatistics. *Economic and Geology*, 58, 1246–1267.

[13] Paciorek, C.J., Yanosky, J.D., Puett, R.C., Laden, F., & Suh, H.H. (2009). Practicle large scale spatio-temporal modeling of particulate matter concentrations. *The Annals of Applied Statistics*, 3(1), 370–379.

[14] Sahu, S.K., Gelfand, A.E, & Holland, D.M. (2006). Spatio-temporal modeling of fine particulate matter. *Journal of Agricultural, Biological and Environmental Statistics*, 11(1), 61–68.

[15] Sampson, P.D., & Guttorp, P. (1992). Nonparametric estimation of non-stationary spatial covariance structure. *Journal of the American Statistical Association*, 87, 108–119.

[16] Yanosky, J.D., Paciorek, C.J., Schwartz, J., Laden, F., Puett, R.C., & Suh, H.H. (2008). Spatio-temporal modeling of chronic PM_{10} exposure for the Nurses' Health Study. *Atmospheric Enviornment*, 42, 4047–4062.

[17] Yu, H.L., Wang, C., & Wu, Y. (2009). An automatic approach to the mean and covariance estimation of spatio-temporal non-stationary processes. In J. Pilz (Ed.), *Proceedings StatGIS 2009*. Milos: OnCD-ROM.